Performance Analysis of Spectral Amplitude Coding-Optical Code Division Multiple Access (SAC-OCDMA) in Free Space Optical Networks with a Multi-wavelength Laser Source

MAJID MOGHADDASI[*,1], AMBALI TAIWO[1], SALEH SEYEDZADEH[2], MOHAMMAD BOROON[1],

SALASIAH HITAM[1] AND SITI BARIRAH AHMAD ANAS[1]

[1]*Wireless and Photonic Networks Research Center of Excellence (WiPNET), Department of Computer and Communication Systems Engineering, Faculty of Engineering, Universiti Putra Malaysia, 43400 UPM Serdang, Selangor, Malaysia*

[2]*Integrated Lightwave Reserach Group, Department of Electrical Engineering, Faculty of Engineering, 50603 University of Malaya, Kuala Lumpur, Malaysia*

*Corresponding author. E-mail address: majidmoghaddasi@ieee.org

ABSTRACT

We present spectral amplitude coding, optical code division multiple access technique in free space optical network utilizing multi-wavelength laser source. Using the simulation software, the system performance is analyzed while the impact of the turbulence is also considered. The simulation is implemented using modified double weight (MDW) code and for 3 users. The results show that using receiver aperture diameter D = 4 cm and beam divergence θ = 1 mrad, transmission distance 2.8, 2.45 and 2.25 km is achievable for weak, moderate and strong turbulence respectively. This distance can be improved if bigger D or smaller θ were utilized. Moreover, it is shown that the increment of turbulence increases jitter, which downgrades system performance.

Keywords—Free space optics (FSO); Wireless optical networks; Multi-wavelength laser; Laser array; Optical code division multiple access (OCDMA); Spectral amplitude coding (SAC)

1 INTRODUCTION

Free space optical network (FSO) is a promising technology, which has advantages such as low cost, free of license and also high speed broadband provision [1]. It is applicable in many areas such as last mile, off shore and rural areas. Also it can be utilized in military and inter-satellite applications. Nonetheless, the system performance can be degraded due to different types of impairments. Absorption and scattering cause significant signal loss. Also, scintillation is the most destructive phenomenon which restricts the system throughput [2] .

On the other hand, multiple access methods are required for most of the communication systems to improve the efficiency of the bandwidth usage. Optical code division multiple access (OCDMA) is a promising method which has attracted many researchers because of its numerous benefits including suitability with bursty traffic networks, flexibility and asynchronous network access capability [3-5]. Furthermore, it can provide a robust security in physical layer [6]. An FSO-CDMA network can combine the advantages of both technologies together. Especially, it has been revealed that OCDMA has robustness against atmospheric degrading factors [7]. Ohtsuki proposed and modeled a FSO-CDMA system for the first time. He used temporal encoding scheme in his work and evaluated system performance for different OCDMA and FSO parameters [8]. His work was followed by many researchers who most of them used temporal or two-dimensional encoding techniques to implement OCDMA. However, because free space as a medium is noisier than fiber, it is better to utilize spectral encoding rather than time variant [9]. Spectral amplitude coding (SAC) is an asynchronous, stable, cost-effective and simple encoding scheme which would be a promising candidate to satisfy this needing. Nevertheless, few investigations have been done in this area [10] and all of them utilized LED as optical source. However LED is not suitable for high speed outdoor FSO networks and laser source is required for this system. Multi-wavelength laser sources are feasible candidates to support dense wavelength division

multiplexing (DWDM) and OCDMA systems due to their ability to produce multiple wavelengths from a single coherent wavelength light source [11, 12]. Recent achievements in such economical multi-wavelength lasers and also considerable enhancements in the production of laser arrays such as cheap vertical-cavity surface-emitting laser (VCSEL) [13] has made the usage of multi-wavelength lasers practical. In [12] SAC-OCDMA in FSO via multi-wavelength source was proposed. With mathematical approach, the authors showed that optical beat interference (OBI) is the dominant noise in SAC-OCDMA with multi-wavelength laser source. They also evaluated the system performance with regards to different parameters including the turbulence effect. In mathematical approach, the influence of many components of the system which exist in an actual system is not considered. To approximate real-world results, for the first time, the SAC-OCDMA in FSO with multi-wavelength laser source with considering the OBI and turbulence effects is implemented using simulation software. Using eye diagram, the role of the turbulence in jitter variations is investigated. Since direct calculation of OBI and Rytov variance were not provided by the software simulator, their values were calculated analytically for each situation (depends on received optical power and bit rate) and added manually to the system.

Along the analysis, several parameters including bit rate, receiver aperture size D, and beam divergence θ were investigated. Also, all influential noises, including OBI, thermal noise, shot noise and relative intensity noise (RIN) as well as FSO channel impairments such as attenuation and scintillation were considered.

2 NOISE PARAMETERS

OBI is one of the main noises in an OCDMA system deploying laser sources [14]. OBI, for SAC-OCDMA with multi-wavelength sources and optical fiber as transmission medium can be attained by [15]

$$i_{OBIb}^2 = 2B_e\tau_c R^2 \left\{ P_r^2 \sum_{j=1}^{W} \left[bx_j + \binom{x_j}{2} \right] + P_r \sum_{j=1}^{W} \left(b + x_j \right) P_j^F \left(\psi P_r \right)^2 + \sum_{j=W+1}^{N} \binom{x_j}{2} + \psi^2 P_r \sum_{j=W+1}^{N} x_j P_j^F \right\} \quad (1)$$

where B_e is electrical bandwidth, R photodetector responsivity, P_r is received optical power per chip, W is weight of utilized code, N is code length, τ_c is the coherence time, ψ is the ratio between the optical powers at the photo detectors in the lower and upper branches in balanced detection and P_j^F is the total produced power due to four-wave mixing (FWM) in fiber. b is a bit value and is equal to 1 if the desired transmitter sends bit 1, otherwise it is 0. Also x_j is number of interfering pulses that are sending bit "1" at jth chip of a particular user. Noting that $\tau_c = \frac{1}{B_o}$ (where B_o is the optical bandwidth) and owing to the absence of FWM effects in FSO, the 2nd and 4th terms in the curly bracket are removed. Thus, OBI formula in FSO is simplified as:

$$i_{OBIb}^2 = \frac{2B_e R^2}{B_o} \left\{ P_r^2 \sum_{j=1}^{W} \left[b.x_j + \binom{x_j}{2} \right] + \left(\psi . P_r \right)^2 \sum_{j=W+1}^{N} \binom{x_j}{2} \right\} \quad (2)$$

Also ψ can be attained by:

$$\psi = \frac{\lambda}{W - \lambda} \quad (3)$$

where λ is the wavelength. The code length of utilized coding technique (MDW) is expressed by [16]

$$N = 3X + \frac{8}{3}\left[\sin\frac{X\pi}{3}\right]^2 \tag{4}$$

where X is number of users in the implemented system.

It is assumed that the number of users is large enough. As a result, the interfering pulse is distributed over all *N* wavelengths evenly and x_j can be replaced by its average value:

$$x_j = \langle x_j \rangle, \quad \forall j \tag{5}$$

In this equation

$$\langle x_j \rangle = \frac{(X-1)W}{2N} \tag{6}$$

On the other hand, to calculate the value of received optical power P_r, the influence of transmission channel impairments should be considered. Several phenomena contribute to the weather impairments, including absorption, scattering and turbulence. Absorption and scattering effects can be grouped into attenuation concept and can be described by Beer law [17]:

$$\tau = \frac{I_0}{I_R} = e^{-\Omega L} \tag{7}$$

where I_0 is launched intensity and I_R is detected intensity at distance *L* and Ω is attenuation coefficient. The equation describes that τ, the transmission radiation is a function of distance

L in the atmosphere. Then received optical power per chip for an SAC-OCDMA can be expressed as [12]

$$P_r = \frac{P_t e^{-\Omega L}}{X} \tag{8}$$

It should be noted that, turbulence is considered as the main impairment in an FSO network, which occurs due to variation in refractive index of the air. Turbulence is measured by refractive index structure coefficient C_n^2 which varies from $10^{-13}m^{-2/3}$ for strong turbulence to $10^{-17}m^{-2/3}$ [18] for weak one. The turbulence includes three phenomena namely beam wandering, scintillation and beam spreading. The dominant factor of the turbulence is scintillation which impacts performance of the system severely [18]. Scintillation effect is characterized by Rytov variance:

$$\sigma_R^2 = 1.23 C_n^2 K^{7/6} L^{11/6} \tag{9}$$

Where $K = \frac{2\pi}{\lambda}$ is the optical wave number.

The value of Rytov variance determines strength of turbulence. $\sigma_R^2 < 1$ indicates weak turbulence, while $\sigma_R^2 = 1$ and $\sigma_R^2 > 1$ indicate moderate and strong turbulence, respectively. With regards to turbulence, since the Rytov variance is not included in the software, it was calculated for each situation based on the distance, refractive index coefficient and was added to the system manually.

Scintillation index is used for measurement of scintillation. It depends on different parameters including wavelength, distance, receiver aperture size and also Rytov variance. Scintillation index is defined as

$$\sigma_I^2 = \left(1+\sigma_x^2\right)\left(1+\sigma_y^2\right)-1 \tag{10}$$

where

$$\sigma_x^2 = e^{\sigma_{\ln x}^2} - 1 \quad ; \quad \sigma_y^2 = e^{\sigma_{\ln y}^2} - 1 \tag{11}$$

where σ_x^2 and σ_y^2 are the normalized variances of irradiance as affected by the large-scale and small-scale turbulent eddies, respectively

$$\sigma_{\ln x}^2 = \frac{0.49\sigma_R^2}{\left(1+0.65d^2+1.11\sigma_R^{12/5}\right)^{7/6}} \tag{12}$$

$$\sigma_{\ln y}^2 = \frac{0.51\sigma_R^2\left(1+0.69\sigma_R^{12/5}\right)^{-5/6}}{1+0.9d^2+0.62d^2\sigma_R^{12/5}} \tag{13}$$

where $d = \sqrt{\frac{K.D^2}{4L}}$

The value of the scintillation index against Rytov variance for signals of different wavelengths and receiver aperture is depicted in Fig. 1:

FIGURE 1 Here

It should be noted that to assess the behavior and influence of the turbulence on the system performance, the Gamma-Gamma model has been utilized by the simulation software. In this model, the probability density function (PDF) of the terms of normalized irradiance I is given by

$$P_G(I) = \frac{2(\alpha\beta)^{\frac{(\alpha+\beta)}{2}}}{\Gamma(\alpha)\Gamma(\beta)} I^{\left[\frac{(\alpha+\beta)}{2}-1\right]} K_{\alpha-\beta}\left(2\sqrt{\alpha\beta I}\right) \tag{14}$$

where $K_m(.)$ is the modified Bessel function of the second kind of order m and $\Gamma(.)$ is the Gamma function. Also α and β are the effective number of small -scale and large scale eddies of the turbulent environment respectively and can be attained by

$$\alpha = \frac{1}{\sigma_x^2} \; ; \beta = \frac{1}{\sigma_y^2} \tag{15}$$

3 SYSTEM DESIGN AND DESCRIPTION

FIGURE 2 Here

The FSO-CDMA system with multi-wavelength laser source was implemented using Optisystem version 10 software and its schematic diagram is illustrated in Fig. 2. Modified double weight (MDW) code [16] is used to produce user signature codes. In this study, the system was implemented for 3 users. Based on the code signature, assigned wavelengths for each user are sent into a Mach-Zehnder modulator to be modulated by data signal. Then the superimposed signals of all users are amplified by an amplifier and sent into the free space channel where the signal is affected by attenuation and turbulence. In the simulation, the Rytov variance, σ_R^2 is not provided directly. However, this parameter is related to the refractive index C_n^2, which is included in the simulation. Referring Eq. (9) the value of K is defined based on the transmission wavelength and σ_R^2 is varied by the values of L. So given a specific value of σ_R^2, the amount of C_n^2 was chosen based on value of L. The receiver which located within the line-of-sight (LOS) will detect the transmitted signal. After decoding and passing from an electrical filter, the primary data is recovered. It should be noted that in this simulation work, the noise of OBI is calculated and accumulated in the signal noise using Matlab component at the receiver. The detail of OBI calculation is presented in section 2.

4 RESULTS AND DISCUSSION

The atmospheric attenuation was considered as 3 dB/km which can be used for hazy weather and transmitted power was set 20 dBm which is maximum allowable value according to eye safety regulation [19]. Other primary values for effective parameters have been brought in Table 1.

TABLE 1 Here

FIGURE 3 Here

In Fig. 3 the performance of the system is evaluated regards with distance and for different turbulence strengths. The Rytov variance was set at three values: 0.05, 1 and 2 for weak, moderate and strong turbulence respectively. For strong turbulence, value 2 was chosen because referring to Fig. 1, for $D = 4$ cm, $\sigma_R^2 = 2$ causes the highest scintillation. Maximum acceptable value for BER was considered 10^{-3} which is threshold for a system using forward error correction (FEC) technique [20]. It can be seen that the proposed system can be implemented in various environments with turbulence from weak to strong. The maximum transmission distance for strong, moderate and weak turbulence is about 2.2, 2.4 and 2.9 km respectively.

FIGURE 4 Here

In Fig. 4, the performance of the system is measured regards with transmission distance and for different bit rates. The graph shows that to achieve BER = 10^{-3}, it is possible to transmit

data up to 2.7 km if the bit rate is 1.25 Gbps, while for 2.5 Gbps, the distance can be exceeded over 2.4 km. On the other hand, 10 Gbps bit rate is not accessible. The reason for this is that both thermal noise and OBI are strongly dependent on the bit rate and are raised with bit rate increment.

FIGURE 5 Here

In Fig. 5 the effect of receiver aperture size on the system performance is observed. As it was mentioned in the previous figure, with $D = 4$ cm, distance 2.4 km is accessible. On the other hand, with $D = 2$ cm, the maximum transmission distance is 1.6 km, while with $D = 8$ cm, the supportable distance, L can be extended until more than 3.2 km. This improvement is due to the fact that referring to Fig. 1, it reduces the scintillation index value and so mitigate turbulence impact. Furthermore, increment of receiver aperture increases the received power.

FIGURE 6 Here

Fig. 6 shows the influence of beam divergence on the system performance. For $\theta = 2$ mrad, it is possible to get reasonable performance with distance 1.6 km. On the other hand, with $\theta = 0.5$ mrad, it is possible to reach distance more than 3.2 km. This is because of the fact that smaller values for θ increases the received power.

FIGURE 7 Here

At the next stage, using eye diagram, the effect of the turbulence on the system performance is assessed for $L = 1.7$ km, $\theta = 0.5$ mrad and bit rate of 2.5 Gbps. At the receiver, $D = 2$

cm was set, because referring to Fig. 1 the scintillation index is higher for smaller receiver aperture. Thus eye diagrams of different turbulences are more differentiable. Fig. 7 (a) shows an eye diagram for weak turbulence with $\sigma_R^2 = 0.05$, Fig. 7(b) for moderate turbulence with $\sigma_R^2 = 1$ and Fig. 7(c) for strong turbulence with $\sigma_R^2 = 2$. As it can be observed higher turbulence induces smaller eye opening and also increment in jitter, which eventuates to degradation in system performance. With a measurement of jitter, it was realized that jitter in weak turbulence (Fig 7(a)) is 0.178 portion of the bit period. Meanwhile, in moderate turbulence (Fig. 7(b)) the jitter is 0.209 and in strong turbulence (Fig. 7(c)), it is 0.2477.

CONCLUSION

In this paper, an SAC-OCDMA system with multi-wavelength laser source was implemented in FSO transmission medium. Then performance of the system for different turbulence strengths, bit rates, receiver aperture size and beam divergence was analyzed. Throughout the analysis, all important noises, including shot, thermal, relative intensity noise and optical beat interference were considered in the analysis. Furthermore, beside attenuation effect in the free space, turbulence was also considered. To ensure high accuracy of the results, the values of OBI and Rytov variance were calculated mathematically and added into the system. It was concluded that with bitrate 2.5 Gbps, it is possible to exceed transmission distance more than 2.2 km for any turbulence conditions. Also it was shown that higher turbulence induces bigger jitter which degrades system performance.

Acknowledgement

This work was supported by Research University Grant Scheme (RUGS) of Universiti Putra Malaysia (project number GP-IPS/2013-9399808).

NOMENCLATURE

b	bit value
B_e	electrical bandwidth (Hz)
B_o	optical bandwidth (Hz)
C_n^2	refractive index structure coefficient ($m^{-2/3}$)
D	receiver aperture diameter (m)
I_0	launched intensity (W/m^2)
i^2_{OBI}	optical beat interference
I_R	detected intensity (W/m^2)
K	optical wave number (1/m)
$K_m(.)$	modified Bessel function
L	transmission distance (m)
N	code length
$P_G(I)$	PDF of the terms of normalized irradiance I
P_j^F	total produced power due to FWM (W)
P_r	received optical power per chip (W)
P_t	total transmitted power (W)
R	photodetector responsivity (A/W)
W	code weight
X	number of users
x_j	number of interfering pulses are sending bit “1” at jth chip

Greek symbols

α	effective number of small -scale
β	effective number of large-scale

$\Gamma(.)$	Gamma function
λ	wavelength (m)
σ_I^2	scintillation index
σ_R^2	Rytov variance
σ_x^2	normalized variances of irradiance (large-scale)
σ_y^2	normalized variances of irradiance (small-scale)
τ	attenuation (dB/km)
τ_c	coherence time (s)
ψ	ratio between the optical powers in the lower and upper branches
Ω	attenuation coefficient (m^{-1})

REFERENCES

[1] Chatzidiamantis N.D, Michalopoulos D.S, Kriezis E.E, Karagiannidis G.K, Schober R. Relay selection protocols for relay-assisted free-space optical systems. *Journal of Optical Communications and Networking* **5**(1) (2013), 92-103.

[2] Ghassemlooy Z, Le Minh H, Rajbhandari S, Perez J, Ijaz M. Performance analysis of ethernet/fast-ethernet free space optical communications in a controlled weak turbulence condition. *Journal of Lightwave Technology.* **30**(13) (2012), 2188-94.

[3] Seyedzadeh S, Mahdiraji , G. A., Sahbudin R. K. Z., Abas A. F., and S. B. A. Anas, Effects of Fiber Dispersion on the Performance of Optical CDMA Systems. *Journal of Optical Communications*" (2012), 311-320.

[4] Huang J-F, Chen K-S, Lin Y-C, Li C-Y. Reconfiguring waveguide-gratings-based M-signature codecs to enhance OCDMA network confidentiality. *Optics Communications*. **313** (2014), 223-30.

[5] Vardakas J., Moscholios I.D., Logothetis M.D. and Stylianakis V.G. Performance Analysis of OCDMA PONs Supporting Multi-Rate Bursty Traffic. *IEEE Transactions on Communications* (2013), 3374 - 3384.

[6] Gao K, Wu C, Sheng X, Shang C, Liu L, Wang J. Optical code division multiple access secure communications systems with rapid reconfigurable polarization shift key user code. *Optical Engineering* **54**(9), (2015) 096101

[7] Yin H. and Richardson D.J. *Optical code division multiple access communication networks: theory and applications.* Southampton: Springer. 2008.

[8] Ohtsuki T. Performance analysis of atmospheric optical PPM CDMA systems. J*ournal of Lightwave Technology* **21**(2), (2003) 406-411.

[9] Ghafouri-Shiraz H. and Karbassian M.M. *Optical CDMA networks: principles, analysis and applications.* Chichester : John Wiley & Sons. 2012.
[10] Moghaddasi M, MaMdoohi G, Noor A.S.M, Hitam S. , Anas A. B. S, Evaluation of OCDMA Encoding Techniques for Free Space Optics, *Lasers in Engineering* **33**(4-6), (2016) 247-260
[11] Wang Z, Wu H, Fan M, Li Y, Gong Y, Rao Y. Broadband flat-amplitude multiwavelength Brillouin-Raman fiber laser with spectral reshaping by Rayleigh scattering. Optics express **21**(24), (2013) 29358-63.
[12] Moghaddasi M, Mamdoohi G, Noor ASM, Mahdi MA, Anas SBA. Development of SAC–OCDMA in FSO with multi-wavelength laser source. *Optics Communications* **356** (2015), 282-9.
[13] Sciancalepore C, Bakir BB, Menezo S, Letartre X, Bordel D, Viktorovitch P. III-V-on-Si photonic crystal vertical-cavity surface-emitting laser arrays for wavelength division multiplexing. *Photonics Technology Letters, IEEE* **25**(12), (2013)1111-3
[14] Tančevski L, Rusch LA. Impact of the beat noise on the performance of 2-D optical CDMA systems. *Communications Letters, IEEE*. **4**(8), (2000) 264-6.
[15] N. Dang NT, Pham AT. Performance analysis of incoherent multi-wavelength OCDMA systems under the impact of four-wave mixing. Optics express. **18**(10), (2010) 9922-33.
[16] Aljunid S, Ismail M, Ramli A, Ali BM, Abdullah MK. A new family of optical code sequences for spectral-amplitude-coding optical CDMA systems. *Photonics Technology Letters, IEEE.* **16**(10), (2004) 2383-5.
[17] Andrews L.C., Phillips R.L. and Hopen C.Y. *Laser beam scintillation with applications.* Washington: SPIE press. 2001.
[18] Willebrand H.A. and Ghuman B.S. *Free Space Optics: Enabling Optical Connectivity in Todays Networks.* Indianapolis: Sams Publishing. 2002
[19] Aladeloba AO, Woolfson MS, Phillips AJ. WDM FSO network with turbulence-accentuated interchannel crosstalk. *Journal of Optical Communications and Networking*. **5**(6), (2013) 641-51.
[20] Wang Z, Zhong W-D, Fu S, Lin C. Performance comparison of different modulation formats over free-space optical (FSO) turbulence links with space diversity reception technique. *Photonics Journal, IEEE*. **1**(6), (2009) 277-85.

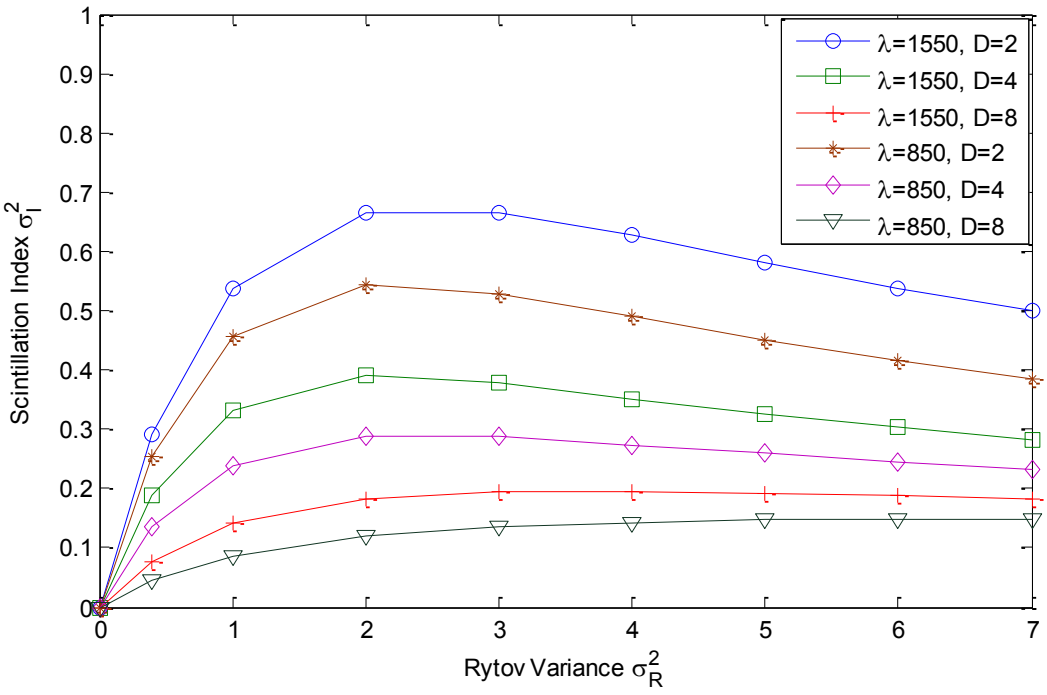

FIGURE 1 Scintillation index as a function of Rytov variance

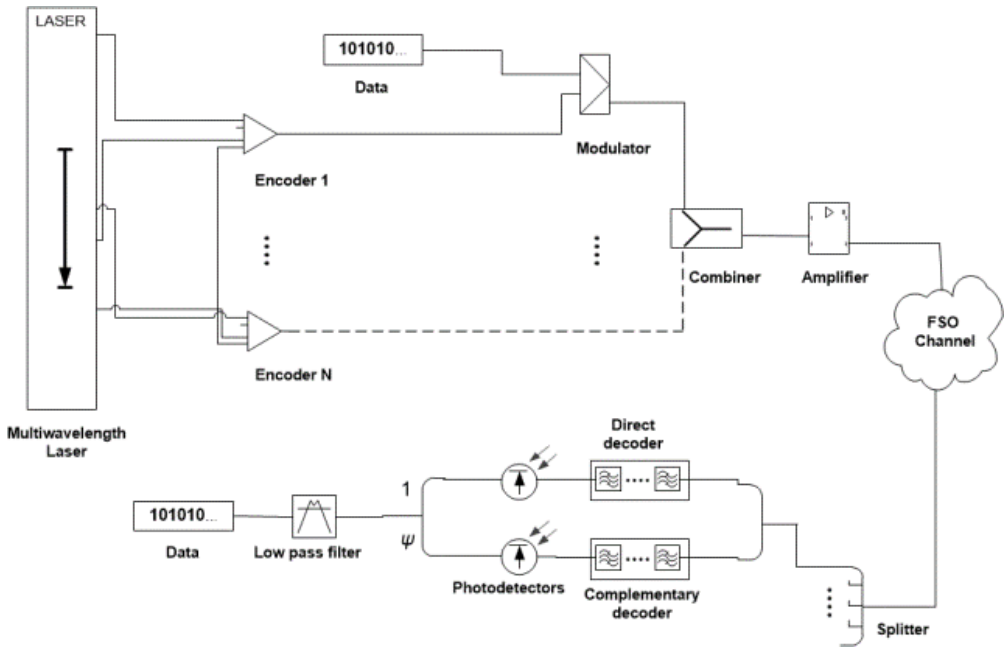

FIGURE 2 Schematic of the transmitter in SAC-OCDMA in FSO

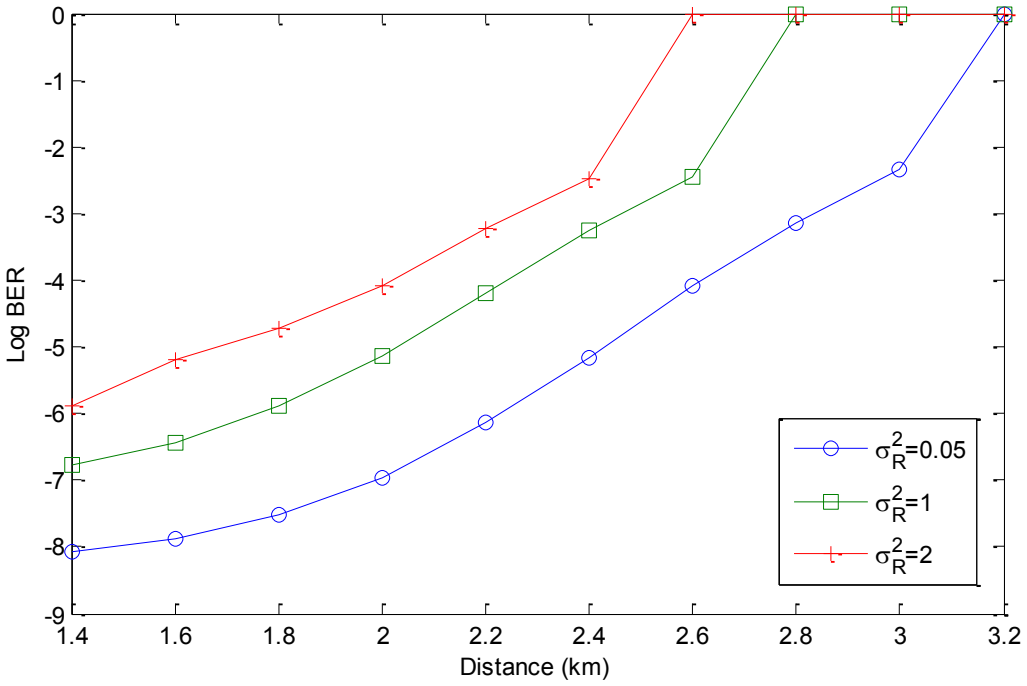

FIGURE 3 Log BER versus distance for different values of turbulence strength

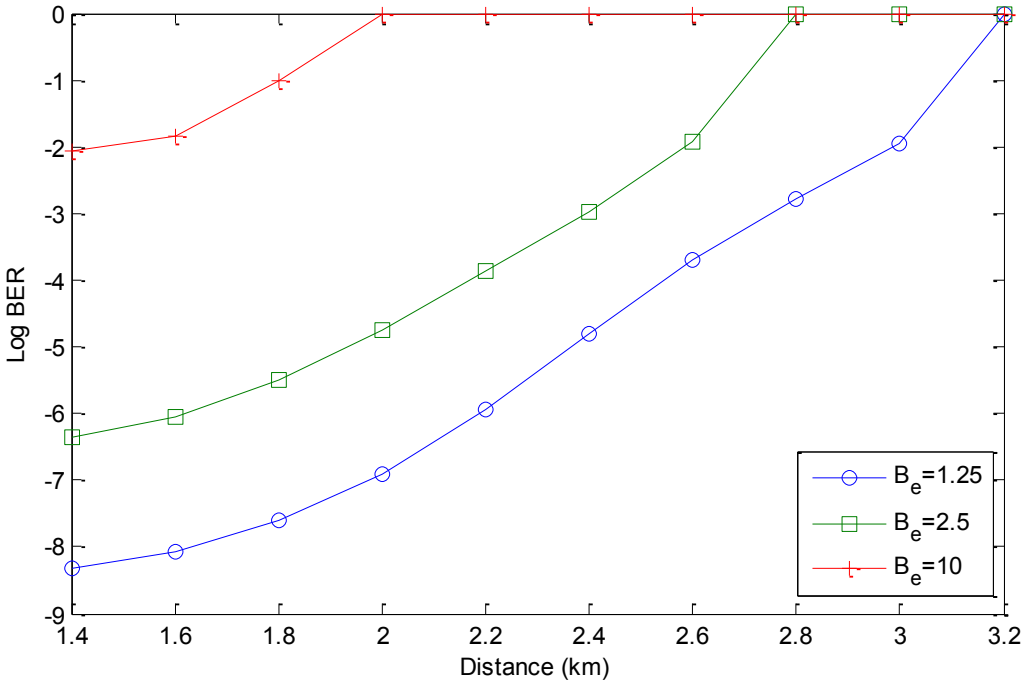

FIGURE 4 Log BER versus distance for different bit rate

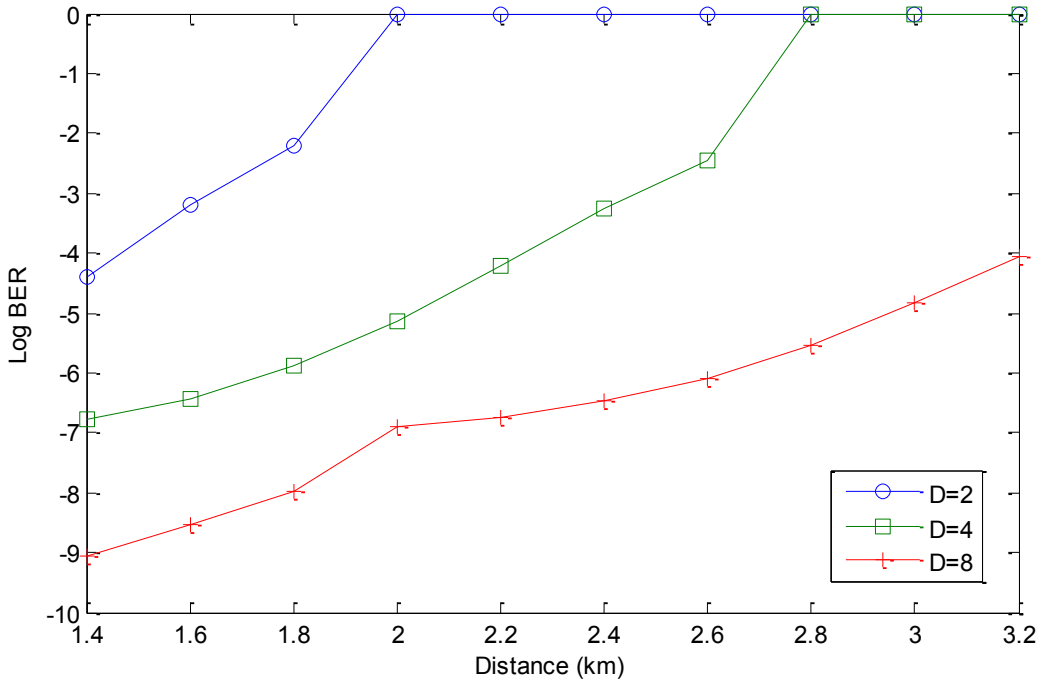

FIGURE 5 Log BER versus distance with different receiver aperture

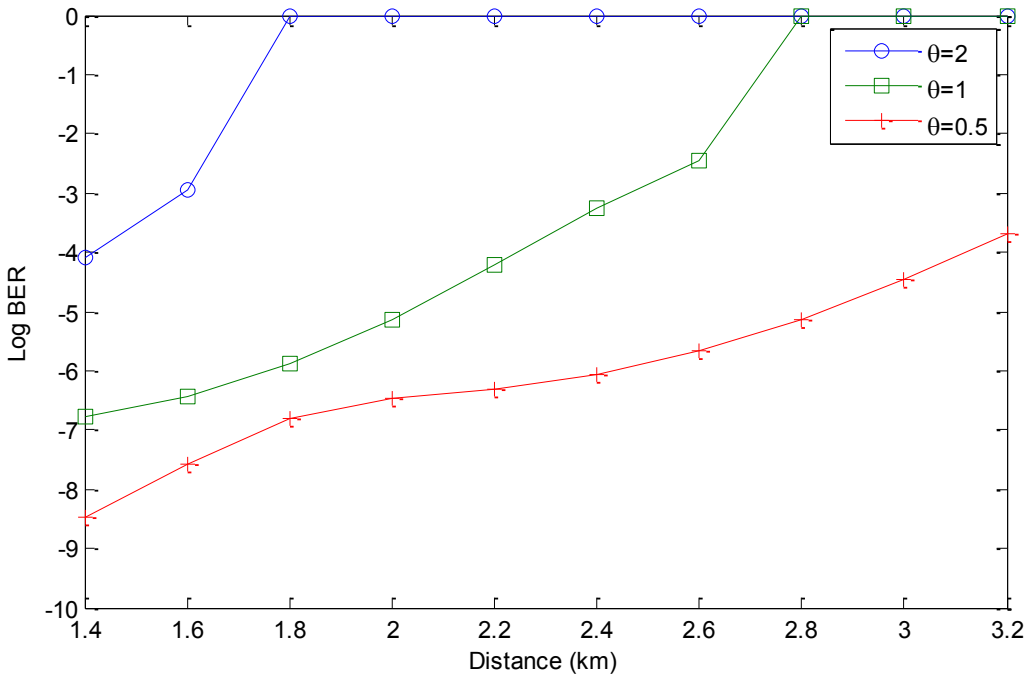

FIGURE 6 Log BER versus distance with different beam divergence

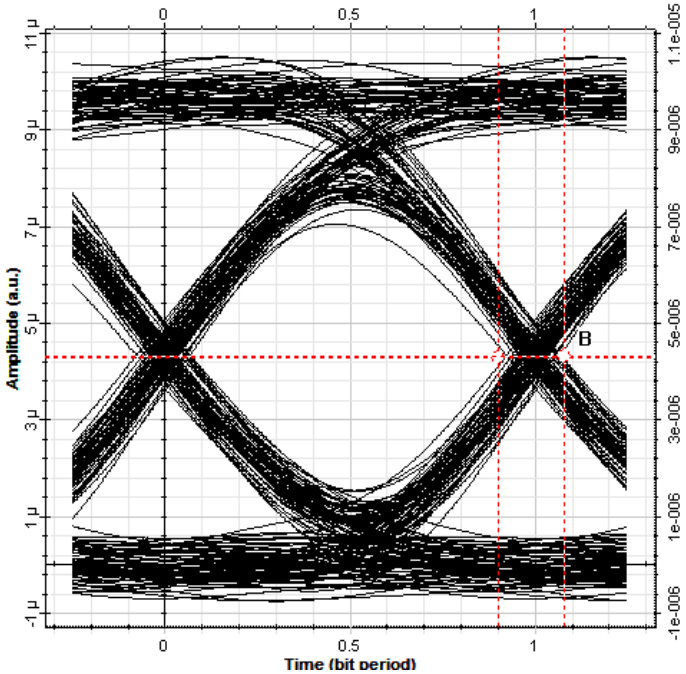
Amplitude (a.u.)
Time (bit period)
B

(a)

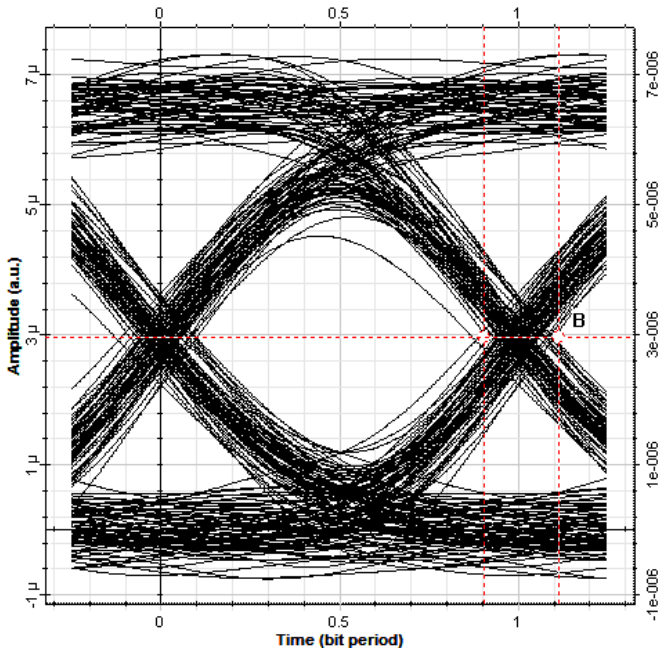
Amplitude (a.u.)
Time (bit period)
B

(b)

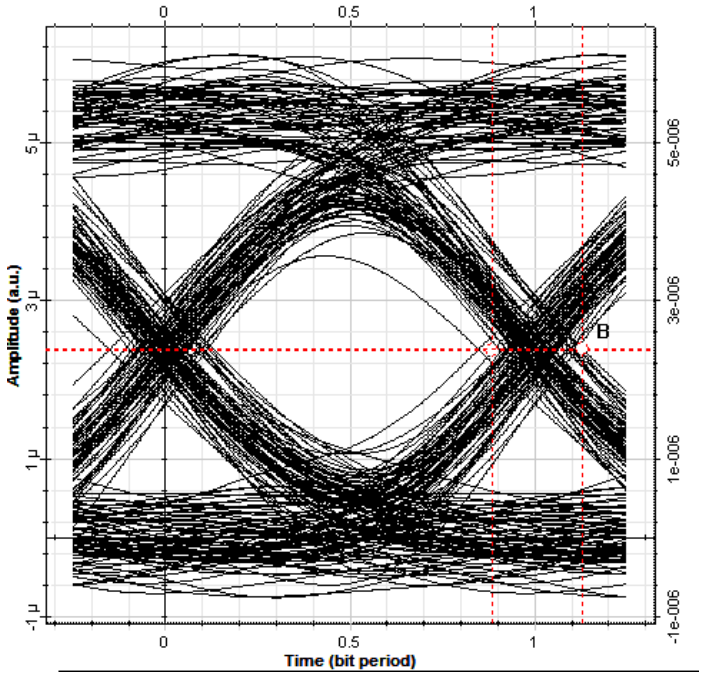

(c)

FIGURE 7 Eye diagram for (a) weak, (b) moderate and (c) strong turbulence

---

TABLE 1 Key parameters used in the simulation

Name	Symbol	Value
Receiver responsivity	R	1
Wavelength	λ	1.55e-6 m
Aperture diameter	D	4 cm
Channel space	Λ	100 GHz
Weather attenuation	Ω	3 dB/km
Bit rate	B_e	2.5 Gbps
Transmission distance	L	1.7 km
RIN noise factor	RIN	-130 $dBHz^{-1}$
Total transmitted power	P_t	20 dBm
Beam divergence	θ	1 milliradians (mrad)